Targeting Endoplasmic Reticulum Stress and Akt with OSU-03012 and Gefitinib or Erlotinib to Overcome Resistance to Epidermal Growth Factor Receptor Inhibitors

Yu-Chieh Wang,[1] Samuel K. Kulp,[1] Dasheng Wang,[1] Chih-Cheng Yang,[1] Aaron M. Sargeant,[1,2] Jui-Hsiang Hung,[1] Yoko Kashida,[1] Mamoru Yamaguchi,[2] Geen-Dong Chang,[3] and Ching-Shih Chen[1]

[1]Division of Medicinal Chemistry and Pharmacognosy, College of Pharmacy, and [2]Department of Veterinary Biosciences, College of Veterinary Medicine, The Ohio State University, Columbus, Ohio; and [3]Institute of Biochemical Sciences, National Taiwan University, Taipei, Taiwan

Abstract

Preexisting and acquired resistance to epidermal growth factor receptor (EGFR) inhibitors limits their clinical usefulness in patients with advanced non–small cell lung cancer (NSCLC). This study characterizes the efficacy and mechanisms of the combination of gefitinib or erlotinib with OSU-03012, a celecoxib-derived antitumor agent, to overcome EGFR inhibitor resistance in three NSCLC cell lines, H1155, H23, and A549. The OSU-03012/EGFR inhibitor combination induced pronounced apoptosis in H1155 and H23 cells, but not in A549 cells, suggesting a correlation between drug sensitivity and basal phospho-Akt levels independently of EGFR expression status. Evidence indicates that this combination facilitates apoptosis through both Akt signaling inhibition and up-regulation of endoplasmic reticulum (ER) stress–induced, GADD153-mediated pathways. For example, ectopic expression of constitutively active Akt significantly attenuated the inhibitory effect on cell survival, and small interfering RNA–mediated knockdown of GADD153 protected cells from undergoing apoptosis in response to drug cotreatments. Furthermore, the OSU-03012/EGFR inhibitor combination induced GADD153-mediated up-regulation of death receptor 5 expression and subsequent activation of the extrinsic apoptosis pathway. It is noteworthy that the ER stress response induced by this combination was atypical in that the cytoprotective pathway was not engaged. In addition, *in vivo* suppression of tumor growth and modulation of intratumoral biomarkers were observed in a H1155 tumor xenograft model in nude mice. These data suggest that the concomitant modulation of Akt and ER stress pathways with the OSU-03012/EGFR inhibitor combination represents a unique approach to overcoming EGFR inhibitor resistance in NSCLC and perhaps other types of cancer with elevated basal Akt activities. [Cancer Res 2008;68(8):2820–30]

Introduction

Lung cancer is the leading cause of cancer mortality in the world (1). Non–small cell lung cancer (NSCLC), which constitutes ~80% of lung cancer cases, is initially responsive to chemotherapy; however, drug-resistant disease ultimately recurs, resulting in a poor prognosis for these patients (2, 3). Efforts to develop novel therapeutic strategies for this disease have led to the approvals of gefitinib and erlotinib, small-molecule inhibitors of epidermal growth factor receptor (EGFR) tyrosine kinase, as third-line therapies for the treatment of patients with advanced NSCLC. Optimism surrounding these targeted agents, however, is tempered by the occurrence of drug resistance that limits their efficacy to 10% to 30% of NSCLC patients (3–6). Extending the clinical usefulness of these EGFR inhibitors to the majority of NSCLC patients who are typically unresponsive will require the elucidation of molecular mechanisms leading to this drug resistance.

Although aberrant overactivation of EGFR can lead to the development and progression of human cancers, activating defects in downstream signaling components can have similar consequences by bypassing normal EGFR-mediated regulation of cell growth and survival. Indeed, functional defects of Ras, Raf, PTEN, and Akt are frequent features of many types of human cancers (7, 8). In lung cancer, overactivation of Akt secondary to loss of PTEN function is well documented (9–11), and recent data indicate a role for hyperactivated phosphatidylinositol 3-kinase (PI3K)/Akt signaling in the resistance to EGFR inhibitors in NSCLC (12–14). These findings suggest that simultaneous inhibition of EGFR and PI3K/Akt pathways may be an effective therapeutic strategy to sensitize resistant NSCLC tumors with aberrant PI3K/Akt signaling to the growth inhibitory and apoptotic effects of the EGFR inhibitors.

OSU-03012, a novel celecoxib derivative that is devoid of cyclooxygenase-2 (COX-2) inhibitory activity, potently induces apoptosis and growth inhibition in cancer cells in association with phosphoinositide-dependent protein kinase-1 (PDK-1) inhibition and subsequent inactivation of Akt and downstream survival signaling pathways (15–17). Recently, the induction of endoplasmic reticulum (ER) stress was also implicated in the antineoplastic effects of OSU-03012. Yacoub et al. (18) observed ER stress responses that were well-correlated with apoptosis in OSU-03012–treated glioblastoma cells, a finding consistent with the strong association between ER stress and apoptosis previously seen in cells treated with nonsteroidal anti-inflammatory drugs, including celecoxib (19). In the present study, we attempt to exploit the multiple antitumor activities of OSU-03012 by testing the hypothesis that treatment with gefitinib or erlotinib in combination with OSU-03012 will overcome resistance to EGFR inhibitors in NSCLC cells through inhibition of Akt signaling and induction of ER stress responses. Our data show that apoptosis induced by the drug combination in gefitinib/erlotinib–resistant

Note: Supplementary data for this article are available at Cancer Research Online (http://cancerres.aacrjournals.org/).

Requests for reprints: Ching-Shih Chen, Division of Medicinal Chemistry and Pharmacognosy, College of Pharmacy, The Ohio State University, 500 West 12th Avenue, Columbus, OH 43210. Phone: 614-688-4008; Fax: 614-688-8556; E-mail: chen.844@osu.edu.

doi:10.1158/0008-5472.CAN-07-1336

NSCLC cells expressing high Akt activity involves alterations in survival pathways downstream of both Akt inhibition and ER stress induction, and that these effects are observed in an *in vivo* xenograft model of EGFR inhibitor–resistant NSCLC in association with suppressed tumor growth.

Materials and Methods

Cell culture and reagents. The human NSCLC cell lines A549 (adenocarcinoma), NCI-H1155 (large cell carcinoma), and NCI-H23 (adenocarcinoma) were obtained from the American Type Culture Collection, and maintained in the suggested complete growth medium. Gefitinib, erlotinib, and celecoxib were prepared from commercial Iressa, Tarceva, and Celebrex tablets, respectively, by solvent extraction followed by recrystallization. OSU-03012 was synthesized according to the procedures previously described (15). For *in vivo* studies, erlotinib and OSU-03012 were prepared as suspensions in vehicle (0.5% methylcellulose, 0.1% Tween 80 in sterile water) for oral administration to tumor-bearing immunocompromised mice. LY294002 was purchased from Sigma-Aldrich. Information on antibodies used in the study is provided in Supplementary Materials and Methods.

Cell viability analysis. A549 and H23 cells were seeded into 96-well plates (5,000 per well), incubated overnight, and treated as indicated for 24 h. Nonadherent H1155 cells (10,000 per well) were directly suspended in drug-containing medium, and incubated for 24 h. Control groups received DMSO vehicle (0.1%, final concentration). After treatment, cells were incubated in medium containing 0.4 mg/mL 3-[4,5-dimethyl- thiazol-2-yl]-2,5-diphenyl-2*H*-tetrazolium bromide (MTT; TCI America) or 3-(4,5-dimethylthiazol-2-yl)-5-(3-carboxymethoxy-phenyl)-2-(4-sulfophenyl)-2*H*-tetrazolium (MTS; Promega) at 37°C for 1 h. Reduced MTT was solubilized in DMSO for determination of absorbance at 570 nm. Absorbance of reduced MTS was directly measured in the reaction medium at 490 nm.

Flow cytometry. Drug-treated cells were analyzed for apoptosis, cell surface expression of DR5 protein, and caspase-8 activity by flow cytometry. A549 and H23 cells were seeded into six-well plates (2×10^5 per well), incubated overnight, and then treated as indicated. H1155 cells (4×10^5) were directly suspended in drug-containing medium. For assessment of apoptosis, cells were collected and stained with Annexin V–Alexa Fluor 488 and propidium iodide according to the vendor's protocols (Molecular Probes). For determination of DR5 expression, cells were incubated in PBS containing phycoerythrin-conjugated antibodies against the extracellular domain of DR5 for 30 min at room temperature. For measurement of caspase-8 activity, cells were incubated with the fluorogenic caspase-8 substrate, 1r-z (AnaSpec), for 20 min. Analyses were performed using a FACSCalibur fluorescence-activated cell sorter (Becton Dickinson Immunocytometry Systems) equipped with CellQuest software.

Western blot analysis. Cell lysates were prepared using acidic lysis buffer (pH 3.4) containing 50 mmol/L bis-(hydroxyethyl)-piperazine, 8 mol/L urea, and 2% CHAPS. Equivalent amounts of proteins were resolved by SDS-PAGE and then transferred to nitrocellulose membranes for immunoblotting as described previously (20). For immunoblotting of biomarkers in xenograft tumors, tumor-tissue homogenates were prepared and immunoblotting was done as described previously (21).

Semiquantitative reverse transcription-PCR. Total RNA was isolated using TRIzol reagent (Invitrogen) and chloroform extraction. The first-strand cDNA was synthesized using the iScript cDNA synthesis kit (Bio-Rad) according to the manufacturer's protocol. Reverse transcription and PCR were performed in a Peltier thermal cycler (PTC-200, MJ Research) using the following primers:

DR5 gene: 5′-GCCTCATGGACAATGAGATAAAGGTGGCT-3′/5′-CACAATCTCAAAGTACGCACAAACGG-3′.

β-actin gene: 5′-ACACTGTGCCCATCTACGAGG-3′/5′-AGGGGCCGGACTCGTCATACT-3′.

Ectopic expression of constitutively active Akt. The pcDNA3.1(+)/ca-Akt plasmid containing cDNA encoding the constitutively active, hemagglutinin-tagged, mutant (T308D/S473D) mouse Akt-1 (CA-Akt) was provided by Dr. Matthew D. Ringel (The Ohio State University, Columbus, OH; ref. 22). Cells were transfected using program A-023 of the AMAXA Nucleofector system according to the manufacturer's instructions. Stable clones expressing the fusion protein were selected from transfected cells using medium containing 250 μg/mL geneticin (Invitrogen-Life Technologies).

GADD153, DR5, and PDK-1 expression knockdown. Knockdowns of GADD153 and DR5 expression were achieved by transfection with the human *DDIT3* SMARTpool small interfering RNA (siRNA) reagent (Dharmacon) and the human *DR5* siRNA reagent (Santa Cruz Biotechnology), respectively. Suppression of PDK-1 expression was achieved by transfection with the HuSH 29mer short hairpin (shRNA) constructs against human *PDPK1* (OriGene Technologies). Cells (2×10^6) were mixed with 250 nmol/L *DDIT3* siRNA, 100 nmol/L *DR5* siRNA, or 4 μg of the shRNA expression constructs and then nucleofected as described above.

Analysis of *DR5* gene promoter activity. The pDR5Pro plasmid containing a cDNA sequence encoding the modified firefly luciferase driven by the *DR5* promoter was constructed by PCR amplification of the 5′ flanking region (−8 to −329) of the *DR5* gene from the genomic DNA of H1155 cells and cloning into a pGL3-basic vector (Promega). Mutations were introduced into the wild-type GADD153-binding sequence of the *DR5* promoter using a site-directed mutagenesis kit (Stratagene) to generate the pDR5Pro-GADD153mt plasmid. Both plasmids were sequenced to confirm the fidelity of construction. The sequences of primers used for plasmid construction and mutagenesis are provided in Supplementary Materials and Methods. H1155 cells were cotransfected with the pDR5Pro or pDR5Pro-GADD153mt plasmid and a Renilla luciferase vector by nucleofection. Cells were treated at the indicated drug concentrations for 12 h, and then assayed for luciferase activities that were measured in a MicroLumatPlus LB96V luminometer (Berthold Technologies). The firefly luciferase activity was normalized to that of Renilla luciferase.

Transmission electron microscopy. H1155 cells (4×10^5 per well; six-well plates) were treated with DMSO, a combination of 3 μmol/L OSU-03012 and 6 μmol/L gefitinib, or 5 μmol/L thapsigargin as a positive control for 8 h. Cells were then fixed in a solution containing 8% paraformaldehyde, 5% glutaraldehyde, 1% tannic acid, and 30 mmol/L sodium cacodylate for 1 h. The fixed cells were suspended in a buffered solution containing 1% osmic acid for 1 h, followed by dehydration in a graded ethanol series, washing with acetone, and embedding into EPON epoxy resin. Ultrathin sections (60–80 nm) were prepared on an ultramicrotome and double-stained with uranyl acetate and lead citrate. All sections were examined and photographed with a Philips EM300 transmission electron microscope.

***In vivo* studies.** Six-week-old female NCr athymic nude mice (National Cancer Institute) were group-housed under conditions of constant photoperiod (12 h light/12 h dark) with *ad libitum* access to sterilized food and water. All experimental procedures using these mice were performed in accordance with protocols approved by the Institutional Animal Care and Use Committee of The Ohio State University.

Each mouse was inoculated s.c. with 5×10^5 H1155 cells in a total volume of 0.1 mL serum-free medium containing 50% Matrigel (BD Biosciences). As tumors became established (mean starting tumor volume, 108.5 ± 8.6 mm^3), mice were randomized to four groups ($n = 10$) that received the following treatments: (*a*) methylcellulose/Tween 80 vehicle, (*b*) OSU-03012 at 100 mg/kg body weight per day, (*c*) erlotinib at 100 mg/kg/d, and (*d*) OSU-03012 plus erlotinib each at 100 mg/kg/d. Mice received treatments by gavage (10 μL/g body weight) for the duration of the study. Tumors were measured weekly using calipers and their volumes calculated using a standard formula: width^2 × length × 0.52. Body weights were measured weekly. At terminal sacrifice, complete necropsies were performed on all mice and tumors were harvested. A portion of each tumor was frozen in liquid nitrogen for Western blotting analysis and the remainder was fixed in 10% formalin for immunohistochemical staining of relevant biomarkers. All other tissues were fixed in 10% formalin for histopathologic examination. Blood from three to four mice from each group was submitted to The Ohio State University Veterinary Clinical Laboratory Services for evaluation of serum chemistry and hematologic variables.

Histopathologic evaluation and immunohistochemistry. Formalin-fixed tumor and visceral tissues from mice were embedded in paraffin by routine procedures. H&E-stained, 4-μm sections of major organs from three animals per group were evaluated microscopically by a veterinary pathologist. The expression of relevant biomarkers in representative sections of tumor tissues was detected by immunohistochemical staining using specific primary antibodies and the EnVision Plus staining kit (Dako) according to the supplier's instructions. The proliferation and apoptotic indices, as determined by proliferating cell nuclear antigen (PCNA) and cleaved caspase-3 immunostaining, respectively, were calculated as the number of immunopositive cells × 100% divided by the total number of cells per ×400 field.

Statistical analysis. The JMP5.0.1 software package (SAS Institute) was used to perform all data analysis. *In vitro* data were analyzed by the Student's *t* test. Survival analysis in the *in vivo* study was performed by the Kaplan-Meier method and log-rank test. Differences were considered significant at $P < 0.05$.

Results

OSU-03012 enhances EGFR inhibitor–induced apoptosis in gefitinib/erlotinib–resistant NSCLC cells that express high levels of phosphorylated Akt. The effects of OSU-03012, gefitinib, and erlotinib on cell survival were assessed in three different gefitinib/erlotinib–resistant NSCLC cell lines—H1155, H23, and A549. As expected, erlotinib and gefitinib were weak inhibitors of viability in all three cell lines with IC_{50} values >10 μmol/L (Fig. 1*A*). In contrast, H1155, H23, and A549 cells were sensitive to the effects of OSU-03012, which caused dose-dependent reductions in cell survival (Fig. 1*A*) and in levels of phosphorylated Akt (Fig. 1*B*). Moreover, these cell lines exhibited differential sensitivities to the cytotoxic effects of OSU-03012 (IC_{50} values of 3.5, 5.3, and 9.1 μmol/L for H1155, H23, and A549, respectively) that correlated with their relative basal levels of phosphorylated Akt (Fig. 1*A*), which was highest in the most sensitive cell line, H1155, and lowest in the least sensitive cell line, A549.

To assess the effect of cotreatment with OSU-03012 and EGFR inhibitors on cell survival, cells were exposed to individual agents or a combination of OSU-03012 with gefitinib or erlotinib at a fixed concentration ratio of 1:2. Flow cytometric analysis of phosphatidylserine externalization as revealed by Annexin V staining showed that cotreatment with OSU-03012 enhanced the ability of EGFR inhibitors to induce apoptosis in H1155 and, to a lesser extent, H23 cells (Fig. 1*C* and *D*). For example, in the presence of 3 μmol/L OSU-03012, representing its IC_{20} as a single agent in H1155 cells, the extent of apoptosis induction by 6 μmol/L gefitinib or erlotinib increased from <5% to 40% relative to the DMSO vehicle control (Fig. 1*C*). In contrast, the combination treatments caused only modest elevations in the numbers of A549 cells undergoing apoptosis, which were much lower than the striking increases in apoptosis seen in the combination-treated H1155 and H23 cells (Fig. 1*D*). Interestingly, the differential sensitivities of these three cell lines to the OSU-03012/EGFR inhibitor combination were well correlated with basal Akt activity, but not with endogenous levels of wild-type EGFR, which is expressed in all of the cell lines used (Fig. 1*A*; ref. 23).

The combination of OSU-03012 and EGFR inhibitor induces the concomitant inhibition of Akt signaling and up-regulation of GADD153. To clarify the mechanism by which OSU-03012 enhanced the antitumor activities of the EGFR inhibitors, we examined the Akt phosphorylation status in treated H1155, H23, and A549 cells (Fig. 2*A*). Although treatment with 3 μmol/L OSU-03012 or 6 μmol/L gefitinib or erlotinib alone for 8 hours failed to notably affect levels of phospho-Akt in H1155 cells, the combination of OSU-03012 with either EGFR inhibitor (concentration ratio, 1:2) reduced the phosphorylation level of Akt in a dose-dependent manner (*top left*). The responses of H23 cells to single-agent treatments and to the OSU-03012/EGFR inhibitor combination were similar to those of the H1155 cells, except that reductions in phospho-Akt levels were not observed until 24 hours of treatment (*bottom panels*). The A549 cells were also sensitive to the suppressive effect of the combination treatment on phospho-Akt levels (*top right*), although they were much less sensitive to apoptosis induction by the combined treatment than the other two cell lines (Fig. 1*D*). To more directly assess the role of PDK-1/Akt pathway inhibition in the apoptotic activity of the OSU-03012/EGFR inhibitor combination, apoptosis was evaluated in H1155 cells treated with EGFR inhibitor alone or in combination with either the PI3K inhibitor LY294002 or shRNA-mediated knockdown of PDK-1. Figure 2*B* (*left*) shows that, although the combination of erlotinib with 20 μmol/L LY294002 reduced phospho-Akt to a level comparable with that of the erlotinib/OSU-03012 combination, the induction of apoptosis was significantly less than that resulting from the erlotinib/OSU-03012 treatment. Similarly, EGFR inhibitor treatment of H1155 cells in which Akt was inactivated by shRNA-mediated PDK1 knockdown failed to induce apoptosis as the OSU-03012/EGFR inhibitor combination did in mock-transfected cells (Fig. 2*B, right*). Knockdown of PDK-1, however, significantly intensified apoptosis induced by OSU-03012 treatment in combination with EGFR inhibitors. Together, these findings suggest that, in addition to Akt signaling, another mechanism governs the sensitivity of NSCLC cells to apoptotic induction after combined treatment with OSU-03012 and erlotinib or gefitinib.

In light of evidence that OSU-03012 induces ER stress responses in glioblastoma cells (18), we evaluated the effects of OSU-03012, gefitinib, and erlotinib alone and in combination on the expression of GADD153, a well-recognized ER stress-inducible transcription factor. As shown in Fig. 2*A*, all three drugs up-regulated GADD153 in H1155 and H23 cells but not in A549 cells. Notably, this elevation of GADD153 expression was dramatically intensified in H1155 and H23 cells after treatment with the indicated drug combinations, but again not in A549 cells. Moreover, the expression of cyclic AMP–responsive element binding protein 2 (CREB2), a positive transcriptional regulator of the *GADD153* gene that is also associated with the ER stress response, paralleled that of GADD153 after the combination treatment in all three cell lines, suggesting an ER stress–induced, CREB2-mediated mechanism for GADD153 up-regulation in the responsive H1155 and H23 cells (Fig. 2*C, right*).

The ER stress response usually includes a cytoprotective function that is mediated through the up-regulation of chaperone proteins, such as GRP78 and GRP94 (Fig. 2*C, left*; ref. 24). It is noteworthy that the ER stress response elicited by the OSU-03012/EGFR inhibitor combination was atypical in this regard in that it failed to induce the cytoprotective arm of the response as indicated by the unchanged expression levels of these chaperone proteins in treated NSCLC cells (Fig. 2*C, right*).

Taken together, these findings suggest that the concomitant suppression of Akt signaling and up-regulation of GADD153 expression underlies the sensitivity of H1155 and H23 cells to the apoptogenic effects of OSU-03012/EGFR inhibitor combinations. To corroborate this premise, we assessed the protective effects of ectopic expression of the constitutively active, T308D/S473D-double mutant Akt (CA-Akt) and siRNA-mediated knockdown of GADD153 expression against the antitumor activity of OSU-03012/EGFR inhibitor combinations in H1155 cells. As shown in Fig. 3*A*,

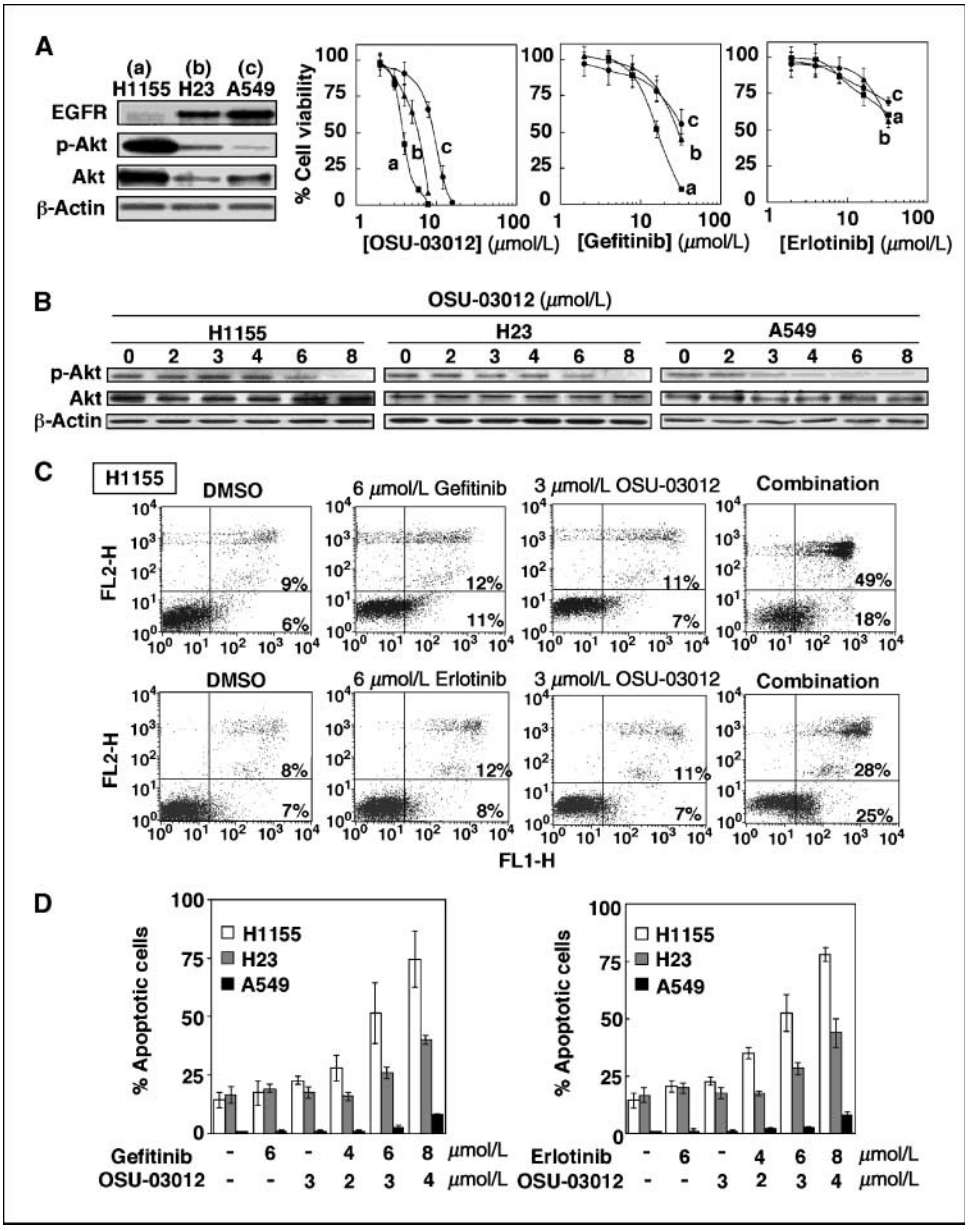

Figure 1. OSU-03012 enhances EGFR inhibitor–induced apoptosis in gefitinib/erlotinib–resistant NSCLC cells that express high levels of phosphorylated Akt. *A,* effects of OSU-03012, gefitinib, or erlotinib on the viability of H1155, H23, and A549 cells. *Right panels,* cells were treated with drugs as indicated for 24 h. Cell viability after drug treatment was determined by the MTT or MTS assay. *Points,* mean of three independent experiments; *bars,* SD. *Left,* basal expression levels of EGFR, ^{473}Ser-Akt, and Akt in H1155, H23, and A549 cells were examined by immunoblotting as described in Materials and Methods. *B,* OSU-03012 dose-dependently decreased phosphorylation of Akt in H1155, H23, and A549 cells. Cells were treated at the indicated concentrations for 8 h and immunoblotting was performed as described in Materials and Methods. *C* and *D,* induction of apoptosis in H1155, H23, and A549 cells treated with OSU-03012 in combination with gefitinib or erlotinib. Cells were treated as indicated for 24 h and assessed for phosphatidylserine externalization by flow cytometry after staining with fluorescence-labeled Annexin V and propidium iodide. Representative quadrantal plots of data from dual-color flow cytometry of treated H1155 cells (*C*). Flow cytometry data were used to determine the percentages of apoptotic H1155, H23, and A549 cells after the indicated treatments (*D*). *Columns,* mean of three independent experiments; *bars,* SD.

the H1155 stable transfectants with highest CA-Akt expression levels (clones 3 and 4; *top left*) were partially, yet significantly, protected from the apoptotic effects of OSU-03012/EGFR inhibitor combinations after 24 hours of treatment compared with the empty vector transfectants ($P < 0.05$; *bottom left* and *right*). Moreover, this protective effect of CA-Akt was also reflected in the phosphorylation status of the Akt substrate, GSK3β, in that the reduction in phospho-GSK3β observed after OSU-03012/EGFR inhibitor treatment was prevented in the CA-Akt transfectants (Fig. 3*A, top right*). Similarly, flow cytometric analysis revealed that siRNA-mediated suppression of GADD153 levels substantially reduced the number of H1155 cells undergoing apoptosis in response to cotreatment with OSU-03012 and gefitinib (Fig. 3*B*).

The combination of OSU-03012 with EGFR inhibitors induces GADD153-mediated up-regulation of death receptor DR5 expression and activates the extrinsic apoptosis pathway. The GADD153 protein is a well-documented regulator of *DR5* gene expression (25, 26). Consequently, the effects of the OSU-03012/EGFR inhibitor combinations on DR5 expression at both the mRNA and protein levels were determined in H1155 cells. As revealed by reverse transcription-PCR (RT-PCR) analysis, treatment with OSU-03012 in combination with either gefitinib or erlotinib for 12 hours dose-dependently elevated DR5 mRNA levels (Fig. 4*A, top panels*). These results were consistent with flow cytometric data showing increased numbers of H1155 cells expressing elevated amounts of cell surface DR5 protein after 24 hours of treatment (Fig. 4*A, bottom panels*).

To establish the involvement of GADD153 in the drug-induced transcriptional up-regulation of *DR5* gene expression, assays using luciferase reporter genes driven by the *DR5* promoter containing either the wild-type or a mutated GADD153-binding sequence were performed. As expected, wild-type *DR5* promoter activity was significantly elevated in H1155 cells treated with the OSU-03012/EGFR inhibitor combinations (Fig. 4*B*). In contrast, mutation of the

GADD153 binding sequence eliminated this drug-induced activation of the *DR5* promoter, strongly indicating that the up-regulation of GADD153 expression in H1155 cells after treatment with the OSU-03012/EGFR inhibitor combinations mediates the associated elevation of DR5 expression.

Next, we sought to establish a link between this drug-induced, GADD153-mediated up-regulation of DR5 expression and the apoptogenic activity of the OSU-03012/EGFR inhibitor combination in NSCLC cells. Because up-regulation and activation of death receptors is associated with the initiation of cancer cell apoptosis, even in the absence of exogenous ligands (25–29), we first assessed indicators of the extrinsic apoptosis pathway as evidence of active DR5 signaling in drug-treated cells. Using a fluorogenic substrate of caspase-8, flow cytometry revealed enhanced caspase-8 activity in H1155 cells treated with OSU-03012 in combination with EGFR inhibitor for 24 hours, compared with those treated with each drug

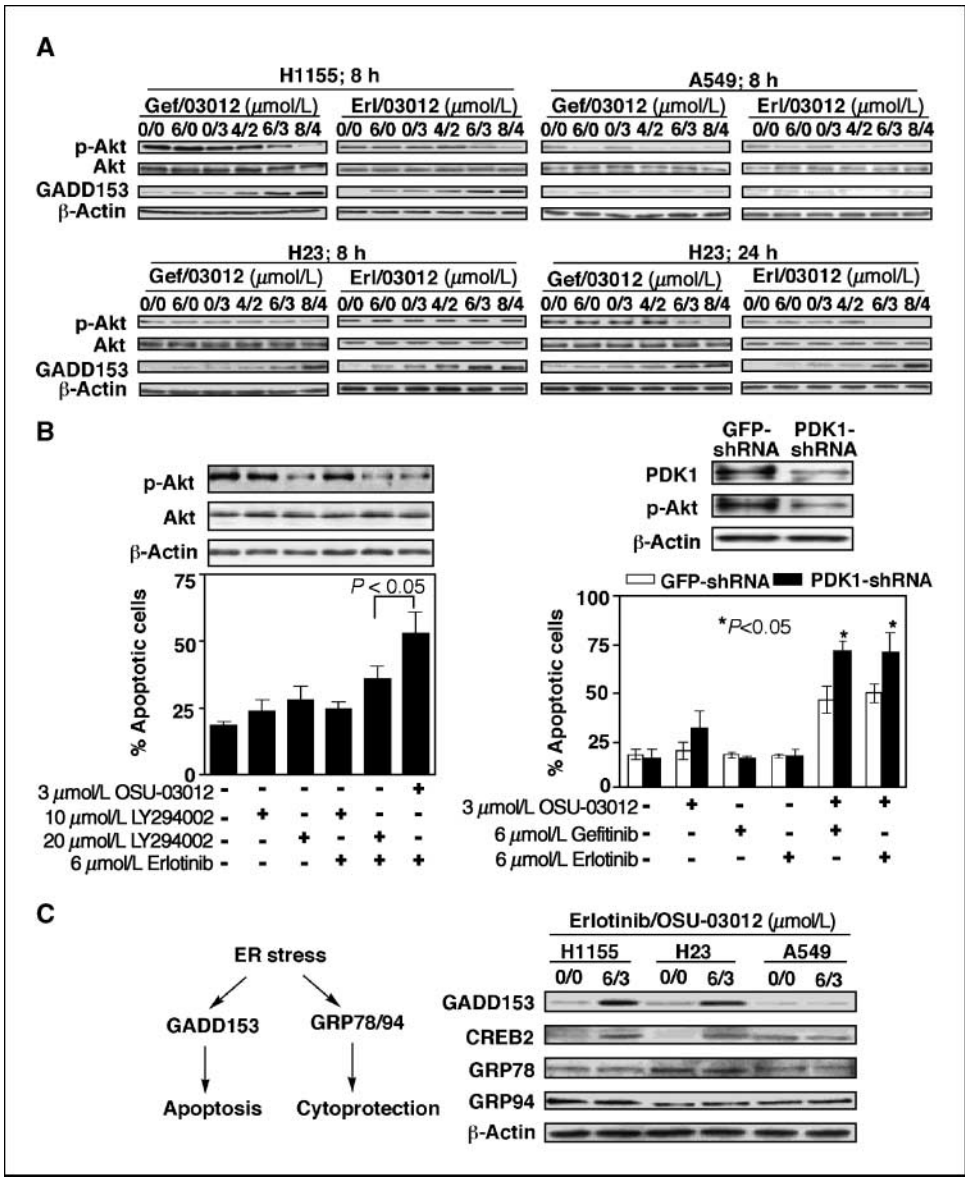

Figure 2. The combination of OSU-03012 with gefitinib or erlotinib induces concomitant inhibition of Akt signaling and up-regulation of ER stress–inducible apoptotic, but not cytoprotective, proteins in H1155 and H23 cells. *A,* effects of combined treatment with OSU-03012 (*03012*) and gefitinib (*Gef*) or erlotinib (*Erl*) on the phosphorylation status of ^{473}Ser-Akt (*p-Akt*) and the expression levels of GADD153 were examined in H1155, H23, and A549 cells. Cells were treated as indicated for 8 or 24 h followed by immunoblotting of cell lysates for the indicated markers as described in Materials and Methods. *B,* effects of PI3K inhibition by LY294002 or shRNA-mediated knockdown of PDK-1 in combination with EGFR inhibitors on apoptosis was assessed in H1155 cells by flow cytometric analysis of phosphatidylserine externalization as described in the Materials and Methods. *Left,* cells were treated with OSU-03012, LY294002, and/or erlotinib at the indicated concentrations for 24 h, and stained with fluorescence-labeled Annexin V and propidium iodide. Effects of treatments on Akt phosphorylation status were examined by immunoblotting (*top*). Percentages of apoptotic cells after the indicated treatments were calculated from flow cytometry data. *Columns,* mean of three independent experiments; *bars,* SD. *Right,* cells were stably transfected with shRNA constructs against human PDK-1 or GFP as controls, treated with OSU-03012, gefitinib, or erlotinib at the indicated concentrations for 24 h, and stained with fluorescence-labeled Annexin V and propidium iodide. Efficiency of PDK-1 knockdown and suppression of phospho-Akt (*p-Akt*) was verified by immunoblotting (*top*). Percentages of apoptotic cells after the indicated treatments were calculated from flow cytometry data. *Columns,* mean of three independent experiments; *bars,* SD (*, $P < 0.05$, Student's *t* test). *C,* the combination of OSU-03012 and erlotinib enhances the expression of proteins in the apoptotic arm, but not the cytoprotective arm, of the ER stress response. Cells were cotreated with 3 μmol/L OSU-03012 and 6 μmol/L erlotinib for 8 h. Immunoblotting was performed as described in Materials and Methods. *Right,* immunoblot of ER stress–inducible proteins, GADD153, CREB2, GRP78, and GRP94, in treated H1155, H23, and A549 cells. *Left,* diagram of apoptotic and cytoprotective signaling pathways of the ER stress response.

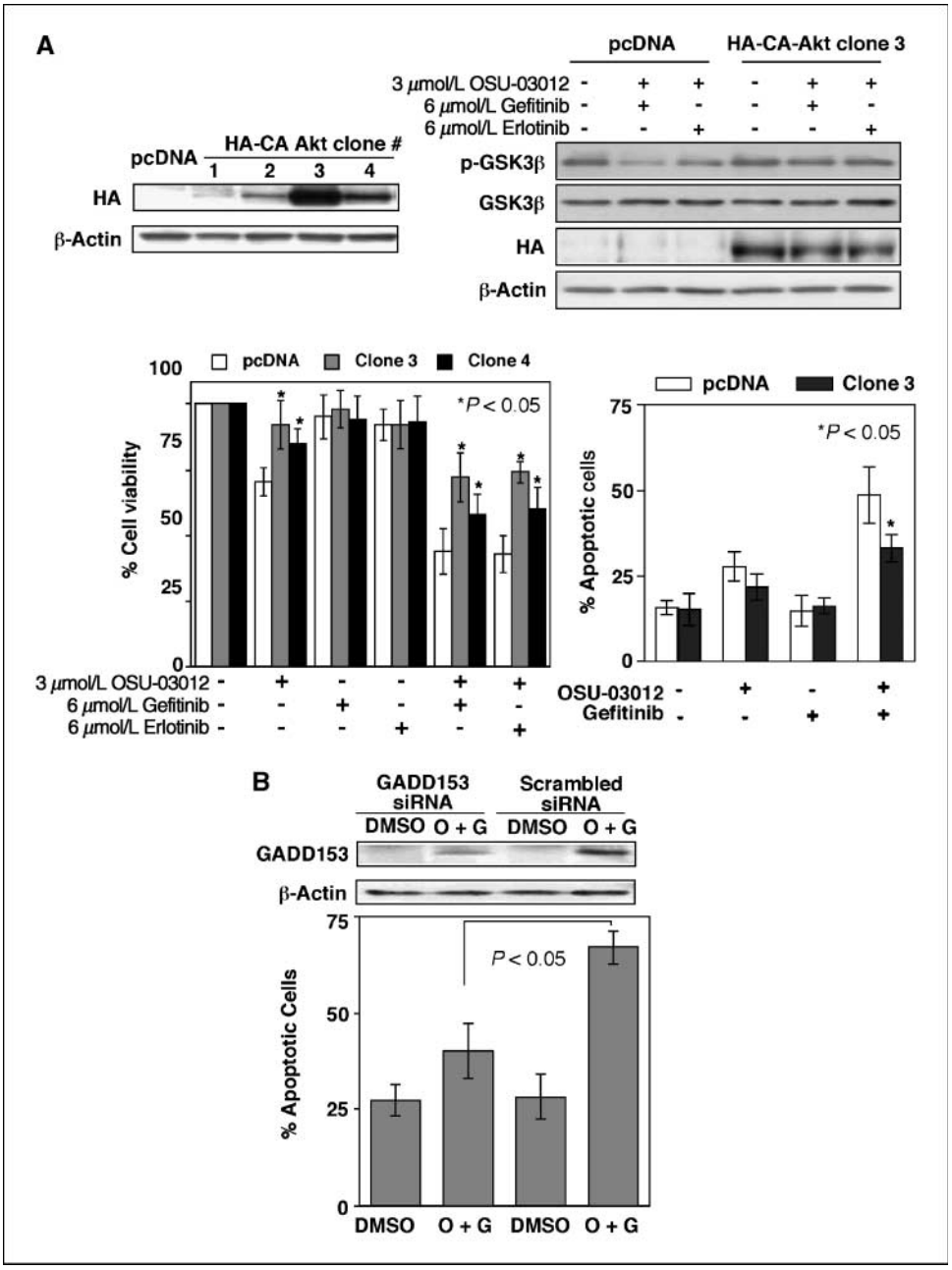

Figure 3. Enforced expression of constitutively active Akt or siRNA-mediated knockdown of GADD153 protects H1155 cells from the apoptotic effects of OSU-03012/EGFR inhibitor combinations. *A,* survival and apoptosis of H1155 cells overexpressing constitutively active Akt were assessed after treatment with the combination of OSU-03012 and gefitinib or erlotinib. Cells were transfected with the expression vector for the constitutively active, hemagglutinin (*HA*)–tagged, mutant (T308D/S473D) mouse Akt-1 (HA-CA Akt). Two stable clones with the highest expression of HA-Akt (*top left*) were treated for 24 h, after which cell viability was determined by the MTS assay (*bottom left*) and, for the higher HA-Akt–expressing clone, apoptosis was assessed by flow cytometry (*bottom right*) as described in Materials and Methods. *Columns,* mean of three independent experiments; *bars,* SD (*, $P < 0.05$, Student's *t* test). *Top right,* constitutively active Akt protects H1155 cells against OSU-03012/EGFR inhibitor–induced dephosphorylation of the Akt substrate, GSK3β. A stable HA-CA Akt–expressing clone was treated with the combination of OSU-03012 and gefitinib or erlotinib as indicated for 24 h and the phosphorylation status of GSK3β was assessed by immunoblotting. *B,* effect of siRNA-mediated knockdown of GADD153 on induction of apoptosis in H1155 cells cotreated with OSU-03012 and gefitinib was assessed by flow cytometric analysis of phosphatidylserine externalization. Cells were transfected with siRNA for the human *DDIT3* gene or scrambled siRNA as controls, treated with OSU-03012 and gefitinib at the indicated concentrations for 24 h, and stained with fluorescence-labeled Annexin V and propidium iodide. Efficiency of GADD153 knockdown was verified by immunoblotting (*top*). Percentages of apoptotic cells after the indicated treatments were calculated from flow cytometry data. *Columns,* mean of three independent experiments; *bars,* SD. *O,* 3 μmol/L OSU-03012; *G,* 6 μmol/L gefitinib.

individually (Fig. 4*C, top* and *middle*). Moreover, this increase in caspase-8 activity was accompanied by enhanced cleavage of Bid (*bottom*). In addition, siRNA-mediated knockdown of DR5 prevented the up-regulation of DR5 mRNA expression observed in H1155 cells after OSU-03012/EGFR inhibitor treatment and significantly reduced the percentage of treated cells undergoing apoptosis (Fig. 4*D*). Together, these findings support a mechanistic framework for the induction of apoptosis in gefitinib/erlotinib–resistant NSCLC cells by OSU-03012/EGFR inhibitor combinations in which the ER stress–inducible transcription factor, GADD153, is induced, leading to up-regulated DR5 expression and stimulation of apoptosis.

Ultrastructural evidence of ER stress in gefitinib/erlotinib–resistant NSCLC cells treated with the combination of OSU-03012 with EGFR inhibitor. Cells undergoing ER stress exhibit characteristic ultrastructural features that can be detected by electron microscopy (30, 31). To verify the induction of ER stress in gefitinib/erlotinib–resistant NSCLC cells by the OSU-03012/EGFR inhibitor combination, H1155 cells were treated with DMSO vehicle, OSU-03012 plus gefitinib, or thapsigargin as a positive control, and then processed for transmission electron microscopy. In contrast to vehicle-treated cells (Fig. 5*A* and *D*), cells treated with OSU-03012/gefitinib (Fig. 5*B* and *E*) or thapsigargin (Fig. 5*C* and *F*) exhibited typical signs of ER stress, including expansion and dilation of the ER as indicated by stacked vacuole-like cytoplasmic structures and thin perinuclear gaps.

Combination treatment with OSU-03012 and erlotinib suppresses the growth of gefitinib/erlotinib–resistant tumor xenografts *in vivo*. To further evaluate the antitumor efficacy of the OSU-03012/EGFR inhibitor combination, athymic nude mice

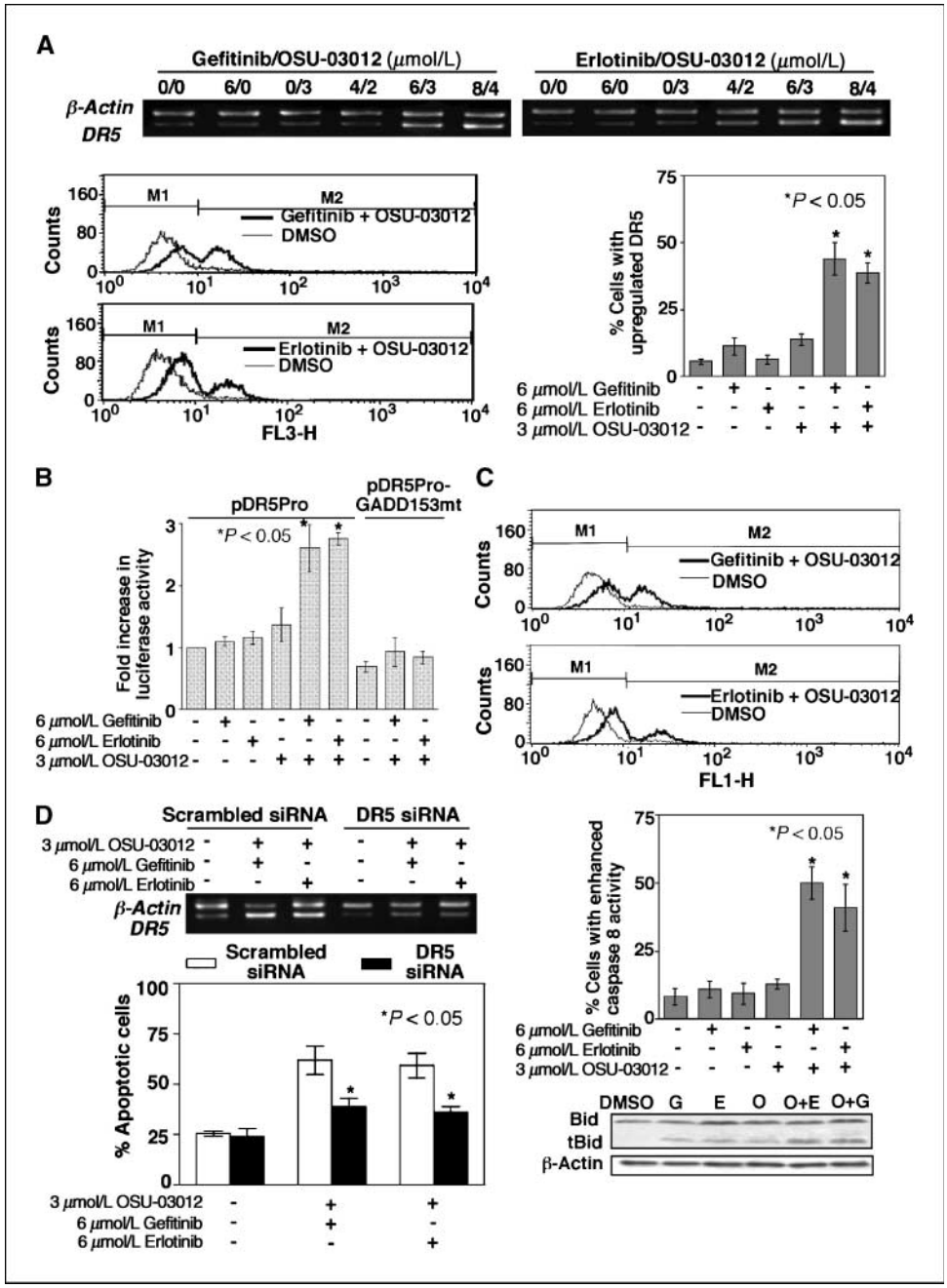

Figure 4. The combination of OSU-03012 with EGFR inhibitors induces GADD153-mediated up-regulation of death receptor DR5 expression and activation of extrinsic apoptosis signaling. *A,* effect of OSU-03012 in combination with gefitinib or erlotinib on mRNA and protein expression levels of the *DR5* gene in H1155 cells. Total RNA was isolated from H1155 cells after treatment with OSU-03012 alone and in combination with erlotinib or gefitinib for 12 h, and then subjected to semiquantitative RT-PCR as described in Materials and Methods (*top left* and *right*). Cells were treated with OSU-03012, gefitinib, or erlotinib alone and in the indicated combinations for 24 h and then stained with phycoerythrin-labeled antibody against the extracellular domain of DR5. Numbers of cells with enhanced fluorescence intensity were determined by flow cytometry (*bottom left*) and expressed as percentages of cells with elevated cell surface expression of DR5 protein (*bottom right*). *Columns,* mean of three independent experiments; *bars,* SD (*, $P < 0.05$, Student's *t* test). *B,* involvement of GADD153 in drug-induced transcriptional up-regulation of *DR5* gene expression was determined by analysis of *DR5* gene promoter activity. H1155 cells were transfected with reporter vectors encoding modified firefly luciferase driven by the wild-type *DR5* promoter (pDR5Pro) or the *DR5* promoter containing a mutated GADD153-binding sequence (pDR5Pro-GADD153mt). Transfectants were treated with drugs as indicated for 12 h and then assayed for luciferase activity as an indicator of reporter gene expression. Firefly luciferase activities were normalized to that of cotransfected Renilla luciferase. *Columns,* mean of three independent experiments; *bars,* SD (*, $P < 0.05$, Student's *t* test). *C,* effect of OSU-03012 in combination with gefitinib or erlotinib on caspase-8 activity and Bid cleavage in H1155 cells. Cells were treated as indicated for 24 h and then, for assessment of caspase-8 activity, incubated with a fluorogenic substrate of caspase-8. Numbers of cells with enhanced fluorescence intensity were determined by flow cytometry (*top*) and expressed as percentages of cells with enhanced caspase-8 activity (*middle*). *Columns,* mean of three independent experiments; *bars,* SD (*, $P < 0.05$, Student's *t* test). For evaluation of Bid cleavage (*bottom*), lysates from treated cells were immunoblotted for intact and truncated Bid (*tBid*) as described in Materials and Methods. *G,* 6 μmol/L gefitinib; *E,* 6 μmol/L erlotinib; *O,* 3 μmol/L OSU-03012. *D,* effect of siRNA-mediated knockdown of GADD153 on induction of apoptosis in H1155 cells cotreated with OSU-03012 and gefitinib or erlotinib was assessed by flow cytometric analysis of phosphatidylserine externalization. Cells transfected with siRNA for the human *DR5* gene or scrambled siRNA as controls were treated as indicated for 24 h, and stained with fluorescence-labeled Annexin V and propidium iodide. The effects of treatments on DR5 mRNA levels (*top*) and apoptosis (*bottom*) in transfected cells were determined by RT-PCR and flow cytometry, respectively. *Columns,* mean of three independent experiments; *bars,* SD (*, $P < 0.05$, Student's *t* test).

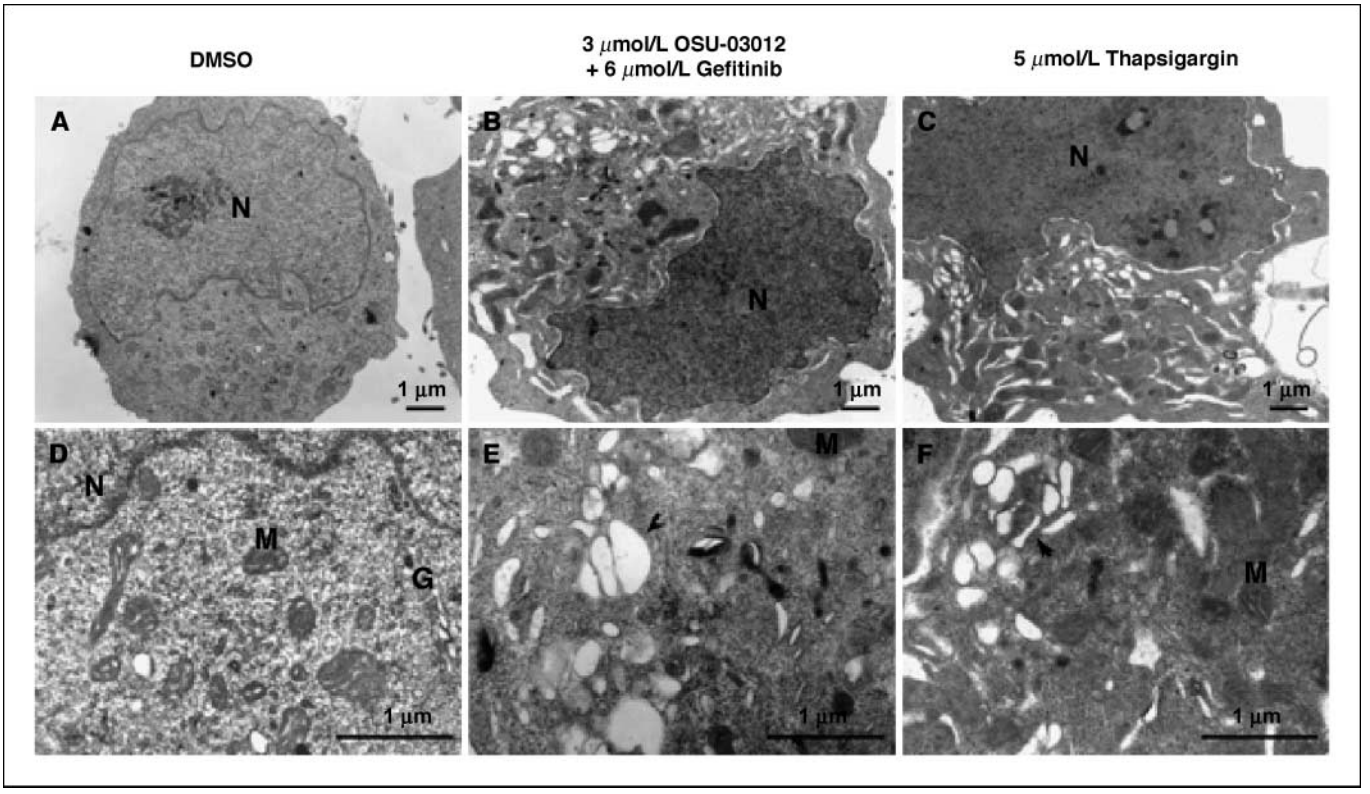

Figure 5. Ultrastructural evidence of ER stress in EGFR inhibitor–resistant NSCLC cells treated with the combination of OSU-03012 and gefitinib. H1155 cells were treated with DMSO (*A* and *D*), the combination of OSU-03012 and gefitinib (*B* and *E*), and thapsigargin as a positive control (*C* and *F*) for 8 h at the indicated concentrations and then visualized by transmission electron microscopy as described in Materials and Methods. *Arrows,* stacked vacuole-like cytoplasmic structures indicative of expanded and dilated ER. *N,* nucleus; *M,* mitochondria; *G,* Golgi apparatus.

bearing established H1155 tumor xenografts were treated orally with OSU-03012 and erlotinib, both alone and in combination, each at 100 mg/kg body weight per day, or with vehicle. Tumor growth was assessed by survival analysis with survival time defined as the time for tumors to reach a volume of 1,200 mm^3. As shown in Fig. 6*A*, the combination treatment significantly prolonged survival, i.e., delayed tumor growth, compared with all other treatments ($P < 0.05$). The estimated mean survival time of mice administered the OSU031012/erlotinib combination was >30 days, whereas the mean survival times of the other groups were <18 days. Moreover, mice tolerated all of the treatments without overt signs of toxicity as indicated by general observations of health, maintenance of body weight, and unremarkable hematology and serum chemistry findings. Centrilobular hepatocellular hypertrophy was observed in mice from both groups receiving OSU-03012 treatments. Aside from this change, which we have reported previously (32), no significant lesions were detected in any tissues from animals subjected to histopathologic examination. To correlate these *in vivo* antitumor effects with mechanisms identified *in vitro*, intratumoral biomarkers of drug activity were assessed by immunohistochemistry and immunoblotting of tumor homogenates. As shown by both techniques, the combination treatment markedly reduced levels of phospho-Akt and elevated levels of GADD153 within tumors (Fig. 6*B*). In addition, immunohistochemical evaluation of PCNA revealed diminished proliferation within tumors from all treatment groups compared with control tumors, whereas assessment of cleaved caspase-3 indicated elevated apoptosis in tumors from mice treated with OSU-03012 alone and in combination with erlotinib (Fig. 6*C*).

Discussion

In this study, we show that combining erlotinib or gefitinib with OSU-03012 potently induces apoptosis in EGFR inhibitor–resistant NSCLC cells. Moreover, we provide evidence that sensitivity of these resistant NSCLC cells to this combinatorial approach correlates with their endogenous levels of phospho-Akt, involves Akt inhibition, and enhances apoptotic signaling downstream of ER stress induction.

Hyperactive Akt signaling has been associated with resistance to EGFR inhibitors in NSCLC, suggesting that combined inhibition of Akt and EGFR signaling represents a rational and promising strategy for overcoming this resistance. Our findings support this contention by showing that treatment of the EGFR inhibitor–resistant H1155 and H23 cell lines with OSU-03012 in combination with gefitinib or erlotinib severely reduced cell survival and enhanced apoptosis in association with diminished phosphorylation of Akt. Moreover, enforced expression of a constitutively active Akt partially but significantly attenuated these inhibitory effects on cell survival, thereby validating Akt signaling as an antitumor target for this drug combination.

Recently, the antitumor activity of OSU-03012 was shown to include the induction of ER stress responses (18). Here we show that, individually, OSU-03012, gefitinib and erlotinib induced ER stress in H1155 and H23 cells as indicated by the nominal upregulation of GADD153. To our knowledge, this is the first report describing the modulation of ER stress–related pathways by erlotinib and gefitinib. In cells treated with the OSU-03012/EGFR inhibitor combination, this elevation of GADD153 expression was

markedly augmented and was associated with increased levels of CREB2, an ER stress–inducible transcriptional regulator of GADD153 expression, and ultrastructural changes indicative of ER stress.

Although the precise molecular mechanism by which these agents, individually and particularly in combination, induce this ER stress response remains incompletely characterized, our data suggest that the effects of gefitinib and erlotinib are independent of EGFR inhibition as indicated by unchanged EGFR autophosphorylation in H23 cells treated with erlotinib at concentrations sufficient to enhance GADD153 expression (Supplementary Fig. S1). Plausible candidates for the off-target effects of gefitinib and erlotinib include proteins potentially involved in ER stress formation, such as HSP90, Lyn, and Fyn, which have been reported

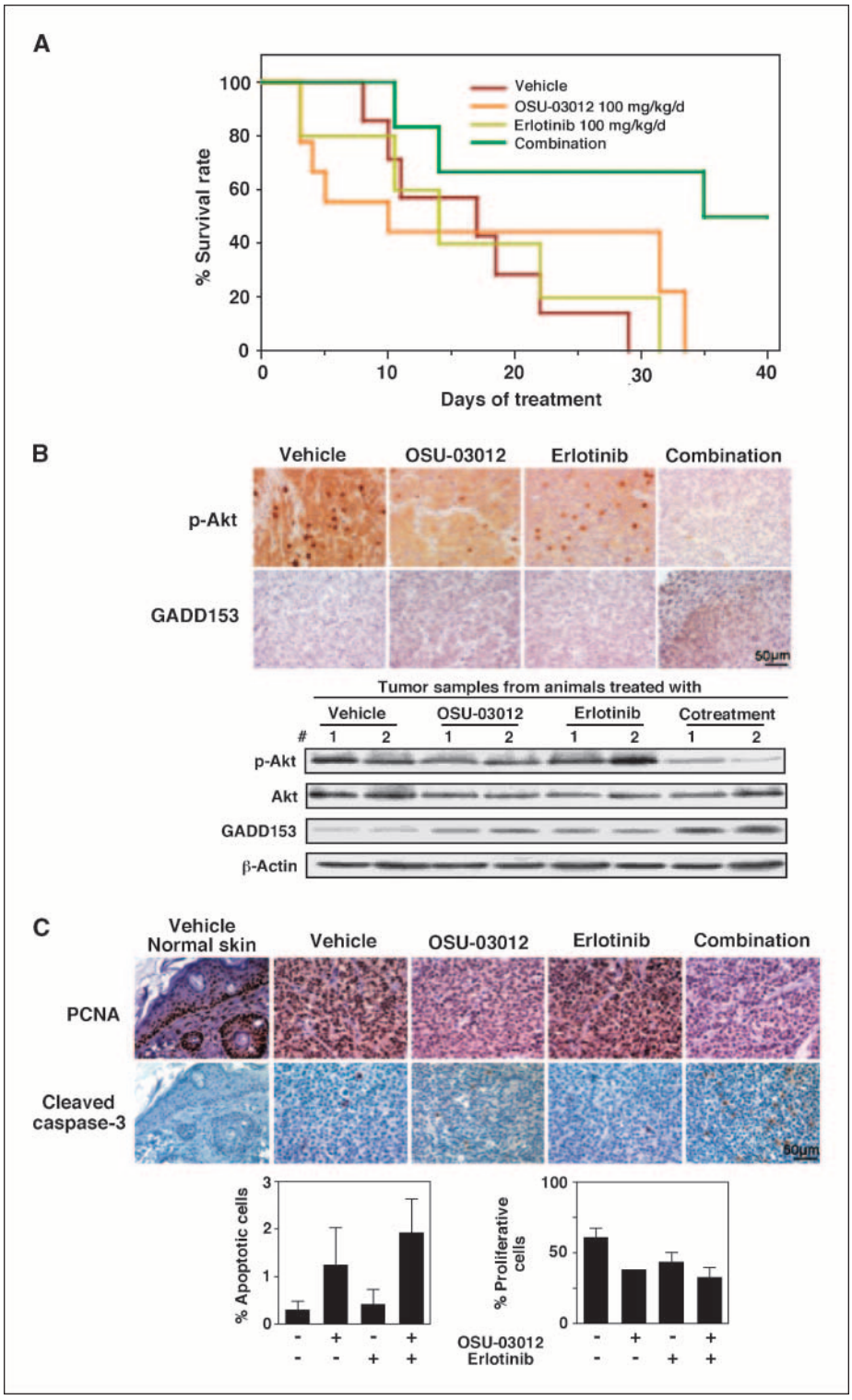

Figure 6. OSU-03012 in combination with erlotinib suppresses the growth of EGFR inhibitor–resistant tumor xenografts *in vivo*. Athymic nude mice bearing established s.c. H1155 xenograft tumors were randomized to four groups (n = 10) that received the following treatments by gavage for the duration of the study: vehicle, OSU-03012 at 100 mg/kg body weight qd, erlotinib at 100 mg/kg qd, or OSU-03012 combined with erlotinib both at 100 mg/kg qd (*Combination*). *A,* Kaplan-Meier survival curves are shown for each treatment group. Survival in the combination group was significantly extended ($P < 0.05$) compared with all other treatment groups. Tumors were measured once per week and survival analysis was performed with survival time defined as the time for tumors to reach 1,200 mm^3. The log-rank test was used to calculate P values. *B,* effects of treatments on intratumoral biomarkers of drug activity in H1155 xenograft tumors. Athymic nude mice bearing established s.c. H1155 xenograft tumors were treated as described above for 2 wk. Tumors were harvested at terminal sacrifice and intratumoral expression of phosphorylated ^{473}Ser-Akt (p-Akt) and GADD153 were examined by immunohistochemistry in formalin-fixed, paraffin-embedded tissues (*top*) and by immunoblotting of the homogenates of two representative H1155 tumors from each treatment group (*bottom*). *C,* immunohistochemical evaluation of intratumoral proliferation and apoptosis in H1155 xenograft tumors. Tumors were harvested from mice treated as described in *B*. Immunostaining for PCNA and cleaved caspase-3 in formalin-fixed, paraffin-embedded tumor tissues was performed, and apoptotic and proliferation indices were calculated as described in Materials and Methods. *Top,* immunohistochemistry showing PCNA and cleaved caspase-3 in H1155 tumors from each treatment group. Normal skin from vehicle-treated mice was included as control. *Bottom,* apoptotic and proliferation indices in H1155 tumors from each treatment group. *Columns,* mean of five ×400 fields; *bars,* SD.

to directly interact with gefitinib (33). Our data also indicate this induction of ER stress to be independent of PDK-1 inhibition, as the suppression of Akt signaling with either the PI3K inhibitor LY294002, or the siRNA-mediated knockdown of PDK-1 could not fully mimic the apoptotic effects of OSU-03012 in combinations with EGFR inhibitors. Disruption of ER calcium homeostasis is a well-documented stimulus for ER stress (34). Consequently, we examined changes in intracellular calcium concentrations in response to treatments with OSU-03012 and gefitinib alone and in combination. A rapid and markedly amplified increase in intracellular calcium concentration was observed after the combination treatment (Supplementary Fig. S2). This finding is reminiscent of that reported for celecoxib, from which OSU-03012 is derived, in prostate cancer cells in which the inhibition of ER Ca^{2+}-ATPases was implicated (35). Moreover, treatment with the OSU-03012/erlotinib combination induced the phosphorylation of protein kinase regulated by RNA-like ER kinase (PERK) and its substrate eIF2α in the responsive H1155 and H23 cells (Supplementary Fig. S3), thereby providing a putative mechanistic link between drug treatment and GADD153 up-regulation. Based on these findings, we hypothesize that perturbation of ER calcium homeostasis is the upstream trigger for activation of PERK/eIF2α signaling, leading to further induction of ER stress responses in cancer cells treated with the OSU-03012/EGFR inhibitor combination. More thorough investigation of this potential mechanism is under way.

Although the precise mechanism by which these agents induce ER stress responses remains undetermined, data from knockdowns of GADD153 and death receptor DR5, and *DR5* promoter analysis provide strong evidence for a mechanistic link between GADD153 up-regulation and the apoptogenic effects of OSU-03012/EGFR inhibitor combinations through activation of the extrinsic apoptosis pathway. Moreover, it is noteworthy that the combination treatments did not up-regulate the cytoprotective chaperones typically associated with ER stress, a finding that distinguishes OSU/EGFR inhibitor combinations from the well-established pharmacologic inducers of ER stress, thapsigargin and tunicamycin.

Celecoxib at supraphysiologic doses induces apoptosis in association with up-regulated expression of ER stress–inducible proteins (19, 36) and death receptor DR5 (37) in a variety of cell types, including NSCLC cells. Our findings using therapeutically achievable concentrations of OSU-03012, a COX-2–inactive celecoxib derivative, suggest that its ability to trigger ER stress represents another COX-2–independent activity in addition to PDK-1/Akt signaling inhibition. The rationale of dual inhibition of COX-2 and EGFR as a therapeutic approach has led to recent phase I trials of celecoxib/EGFR inhibitor combinations for the treatment of head and neck cancer and NSCLC (38, 39). Evidence presented here suggests that OSU-03012 represents a feasible alternative in such combinations through its potent COX-2–independent effects on both Akt signaling and ER stress–mediated apoptotic pathways. The *in vivo* efficacy of the OSU-03012/erlotinib combination was shown in a H1155 tumor xenograft model in which tumor growth was significantly inhibited in association with diminished phospho-Akt and elevated GADD153 levels within tumors and in the absence of limiting toxicities.

In the current study, the EGFR inhibitor/OSU-03012 combinations were assessed *in vitro* at a fixed 2:1 ratio using 6 and 3 μmol/L concentrations, respectively, which were selected for proof-of-principle mechanistic studies based on the results of preceding dose-range experiments (Figs. 1*D* and 2*A*). Although the 6 μmol/L concentration used for the EGFR inhibitors is greater than the average steady-state plasma levels of gefitinib and erlotinib achieved in cancer patients (40–45), this concentration is within the range of reported peak plasma concentrations for erlotinib (44, 46–48). Moreover, induction of apoptosis, GADD153 expression, and DR5 expression were still observed after treatment with the erlotinib/OSU-03012 combination at the lower doses of 4 and 2 μmol/L, respectively.

Based on our findings, parallel suppression of Akt signaling and ER stress–mediated up-regulation of GADD153 expression underlies the sensitivity of H1155 and H23 cells to cotreatment with OSU-03012 and EGFR inhibitors. However, A549 cells were found to be extremely insensitive to the OSU-03012/EGFR inhibitor combination. The differential responsiveness among these cell lines to this combination, as well as to OSU-03012 alone, was strongly correlated with basal levels of phosphorylated Akt, but not with wild-type EGFR expression level. The more sensitive cells, H1155 and H23, exhibited much higher levels of phospho-Akt, likely due to a nonsense mutation in the *PTEN* gene (49, 50), whereas A549 contained the lowest level. This finding suggests a greater dependence of H1155 and H23 cells on Akt signaling for survival and resistance to EGFR inhibitors. Alternatively, the OSU-03012/EGFR inhibitor combination may engage additional apoptotic pathway(s) in the sensitive H1155 and H23 cells that are not induced in A549 cells. Our results suggest that ER stress is this alternative pathway as A549 cells failed to generate an ER stress response after the combination treatment. Moreover, the finding that Akt activity is a determinant of responsiveness to this drug combination is clinically significant in that it may provide a means of selecting patients with EGFR inhibitor–resistant NSCLC tumors that are more likely to respond to this strategy.

The data reported here offer evidence for the efficacy of a unique, combinatorial approach to overcome EGFR inhibitor resistance in NSCLC. This strategy targets both the Akt signaling pathway and the ER stress response, which underlies its potent *in vitro* and *in vivo* antitumor effects and suggests its viability as a therapeutic strategy for the treatment of EGFR inhibitor–resistant NSCLC.

Acknowledgments

Received 4/10/2007; revised 11/19/2007; accepted 2/7/2008.

Grant support: USPHS grant CA112250 from the National Cancer Institute, and a grant from the William R. Hearst Foundation (C-S. Chen).

The costs of publication of this article were defrayed in part by the payment of page charges. This article must therefore be hereby marked *advertisement* in accordance with 18 U.S.C. Section 1734 solely to indicate this fact.

We thank Drs. Roger Briesewitz and Miguel Villalona-Calero (The Ohio State University) for valuable advice, and Drs. Ya-Ting Yang (The Scripps Research Institute) and Chang-Shi Chen (University of California, San Diego) for technical help.

References

1. Parkin DM, Bray F, Ferlay J, Pisani P. Global cancer statistics, 2002. CA Cancer J Clin 2005;55:74–108.

2. Klastersky J, Paesmans M. Response to chemotherapy, quality of life benefits and survival in advanced non-small cell lung cancer: review of literature results. Lung Cancer 2001;34 Suppl 4:S95–101.

3. Maione P, Gridelli C, Troiani T, Ciardiello F. Combining targeted therapies and drugs with multiple targets in the treatment of NSCLC. Oncologist 2006;11:274–84.

4. Brown ER, Shepherd FA. Erlotinib in the treatment of non-small cell lung cancer. Expert Rev Anticancer Ther 2005;5:767–75.
5. Kobayashi S, Boggon TJ, Dayaram T, et al. EGFR mutation and resistance of non-small-cell lung cancer to gefitinib. N Engl J Med 2005;352:786–92.
6. Tsao MS, Sakurada A, Cutz JC, et al. Erlotinib in lung cancer - molecular and clinical predictors of outcome. N Engl J Med 2005;353:133–44.
7. Shaw RJ, Cantley LC. Ras, PI(3)K and mTOR signalling controls tumour cell growth. Nature 2006;441:424–30.
8. Ogawa K, Sun C, Horii A. Exploration of genetic alterations in human endometrial cancer and melanoma: distinct tumorigenic pathways that share a frequent abnormal PI3K/AKT cascade. Oncol Rep 2005;14:1481–5.
9. Marsit CJ, Zheng S, Aldape K, et al. PTEN expression in non-small-cell lung cancer: evaluating its relation to tumor characteristics, allelic loss, and epigenetic alteration. Hum Pathol 2005;36:768–76.
10. Soria JC, Lee HY, Lee JI, et al. Lack of PTEN expression in non-small cell lung cancer could be related to promoter methylation. Clin Cancer Res 2002; 8:1178–84.
11. Tang JM, He QY, Guo RX, Chang XJ. Phosphorylated Akt overexpression and loss of PTEN expression in non-small cell lung cancer confers poor prognosis. Lung Cancer 2006;51:181–91.
12. Kokubo Y, Gemma A, Noro R, et al. Reduction of PTEN protein and loss of epidermal growth factor receptor gene mutation in lung cancer with natural resistance to gefitinib (IRESSA). Br J Cancer 2005;92: 1711–9.
13. Brognard J, Clark AS, Ni Y, Dennis PA. Akt/protein kinase B is constitutively active in non-small cell lung cancer cells and promotes cellular survival and resistance to chemotherapy and radiation. Cancer Res 2001;61:3986–97.
14. Janmaat ML, Kruyt FA, Rodriguez JA, Giaccone G. Response to epidermal growth factor receptor inhibitors in non-small cell lung cancer cells: limited antiproliferative effects and absence of apoptosis associated with persistent activity of extracellular signal-regulated kinase or Akt kinase pathways. Clin Cancer Res 2003;9: 2316–26.
15. Zhu J, Huang JW, Tseng PH, et al. From the cyclooxygenase-2 inhibitor celecoxib to a novel class of 3-phosphoinositide-dependent protein kinase-1 inhibitors. Cancer Res 2004;64:4309–18.
16. Johnson AJ, Smith LL, Zhu J, et al. A novel celecoxib derivative, OSU03012, induces cytotoxicity in primary CLL cells and transformed B-cell lymphoma cell line via a caspase- and Bcl-2-independent mechanism. Blood 2005;105:2504–9.
17. Li J, Zhu J, Melvin WS, Bekaii-Saab TS, Chen CS, Muscarella P. A structurally optimized celecoxib derivative inhibits human pancreatic cancer cell growth. J Gastrointest Surg 2006;10:207–14.
18. Yacoub A, Park MA, Hanna D, et al. OSU-03012 promotes caspase-independent but PERK-, cathepsin B-, BID-, and AIF-dependent killing of transformed cells. Mol Pharmacol 2006;70:589–603.
19. Tsutsumi S, Gotoh T, Tomisato W, et al. Endoplasmic reticulum stress response is involved in nonsteroidal anti-inflammatory drug-induced apoptosis. Cell Death Differ 2004;11:1009–16.
20. Chen CS, Weng SC, Tseng PH, Lin HP. Histone acetylation-independent effect of histone deacetylase inhibitors on Akt through the reshuffling of protein phosphatase 1 complexes. J Biol Chem 2005;280: 38879–87.
21. Kulp SK, Yang YT, Hung CC, et al. 3-phosphoinositide-dependent protein kinase-1/Akt signaling represents a major cyclooxygenase-2-independent target for celecoxib in prostate cancer cells. Cancer Res 2004;64: 1444–51.
22. Saji M, Vasko V, Kada F, Allbritton EH, Burman KD, Ringel MD. Akt1 contains a functional leucine-rich nuclear export sequence. Biochem Biophys Res Commun 2005;332:167–73.
23. Conde E, Angulo B, Tang M, et al. Molecular context of the EGFR mutations: evidence for the activation of mTOR/S6K signaling. Clin Cancer Res 2006;12:710–7.
24. Li J, Lee AS. Stress induction of GRP78/BiP and its role in cancer. Curr Mol Med 2006;6:45–54.
25. Yamaguchi H, Wang HG. CHOP is involved in endoplasmic reticulum stress-induced apoptosis by enhancing DR5 expression in human carcinoma cells. J Biol Chem 2004;279:45495–502.
26. Abdelrahim M, Newman K, Vanderlaag K, Samudio I, Safe S. 3,3′-Diindolylmethane (DIM) and its derivatives induce apoptosis in pancreatic cancer cells through endoplasmic reticulum stress-dependent upregulation of DR5. Carcinogenesis 2006;27:717–28.
27. Aragane Y, Kulms D, Metze D, et al. Ultraviolet light induces apoptosis via direct activation of CD95 (Fas/APO-1) independently of its ligand CD95L. J Cell Biol 1998;140:171–82.
28. Horinaka M, Yoshida T, Shiraishi T, et al. Luteolin induces apoptosis via death receptor 5 upregulation in human malignant tumor cells. Oncogene 2005;24: 7180–9.
29. Kazhdan I, Marciniak RA. Death receptor 4 (DR4) efficiently kills breast cancer cells irrespective of their sensitivity to tumor necrosis factor-related apoptosis-inducing ligand (TRAIL). Cancer Gene Ther 2004;11: 691–8.
30. Nawrocki ST, Carew JS, Pino MS, et al. Bortezomib sensitizes pancreatic cancer cells to endoplasmic reticulum stress-mediated apoptosis. Cancer Res 2005; 65:11658–66.
31. Tiwari M, Kumar A, Sinha RA, et al. Mechanism of 4-HPR-induced apoptosis in glioma cells: evidences suggesting role of mitochondrial-mediated pathway and endoplasmic reticulum stress. Carcinogenesis 2006;27: 2047–58.
32. Sargeant A, Klein R, Rengel R, et al. Chemotherapeutic and bioenergetic signaling effects of PDK-1/Akt pathway inhibition in a transgenic mouse model of prostate cancer. Toxicol Pathol 2007;35:549–61.
33. Brehmer D, Greff Z, Godl K, et al. Cellular targets of gefitinib. Cancer Res 2005;65:379–82.
34. Kaufman RJ. Stress signaling from the lumen of the endoplasmic reticulum: coordination of gene transcriptional and translational controls. Genes Dev 1999;13: 1211–33.
35. Johnson AJ, Hsu AL, Lin HP, Song X, Chen CS. The cyclo-oxygenase-2 inhibitor celecoxib perturbs intracellular calcium by inhibiting endoplasmic reticulum Ca^{2+}-ATPases: a plausible link with its anti-tumour effect and cardiovascular risks. Biochem J 2002;366:831–7.
36. Kim SH, Hwang CI, Park WY, Lee JH, Song YS. GADD153 mediates celecoxib-induced apoptosis in cervical cancer cells. Carcinogenesis 2006;27:1961–9.
37. Liu X, Yue P, Zhou Z, Khuri FR, Sun SY. Death receptor regulation and celecoxib-induced apoptosis in human lung cancer cells. J Natl Cancer Inst 2004;96: 1769–80.
38. Reckamp KL, Krysan K, Morrow JD, et al. A phase I trial to determine the optimal biological dose of celecoxib when combined with erlotinib in advanced non-small cell lung cancer. Clin Cancer Res 2006;12: 3381–8.
39. Wirth LJ, Haddad RI, Lindeman NI, et al. Phase I study of gefitinib plus celecoxib in recurrent or metastatic squamous cell carcinoma of the head and neck. J Clin Oncol 2005;23:6976–81.
40. Swaisland H, Laight A, Stafford L, et al. Pharmacokinetics and tolerability of the orally active selective epidermal growth factor receptor tyrosine kinase inhibitor ZD1839 in healthy volunteers. Clin Pharmacokinet 2001;40:297–306.
41. Herbst RS, Maddox AM, Rothenberg ML, et al. Selective oral epidermal growth factor receptor tyrosine kinase inhibitor ZD1839 is generally well-tolerated and has activity in non-small-cell lung cancer and other solid tumors: results of a phase I trial. J Clin Oncol 2002; 20:3815–25.
42. Baselga J, Rischin D, Ranson M, et al. Phase I safety, pharmacokinetic, and pharmacodynamic trial of ZD1839, a selective oral epidermal growth factor receptor tyrosine kinase inhibitor, in patients with five selected solid tumor types. J Clin Oncol 2002;20: 4292–302.
43. Hidalgo M, Siu LL, Nemunaitis J, et al. Phase I and pharmacologic study of OSI-774, an epidermal growth factor receptor tyrosine kinase inhibitor, in patients with advanced solid malignancies. J Clin Oncol 2001; 19:3267–79.
44. Tan AR, Yang X, Hewitt SM, et al. Evaluation of biologic end points and pharmacokinetics in patients with metastatic breast cancer after treatment with erlotinib, an epidermal growth factor receptor tyrosine kinase inhibitor. J Clin Oncol 2004;22:3080–90.
45. Townsley CA, Major P, Siu LL, et al. Phase II study of erlotinib (OSI-774) in patients with metastatic colorectal cancer. Br J Cancer 2006;94:1136–43.
46. Messersmith WA, Laheru DA, Senzer NN, et al. Phase I trial of irinotecan, infusional 5-fluorouracil, and leucovorin (FOLFIRI) with erlotinib (OSI-774): early termination due to increased toxicities. Clin Cancer Res 2004;10:6522–7.
47. Petty WJ, Dragnev KH, Memoli VA, et al. Epidermal growth factor receptor tyrosine kinase inhibition represses cyclin D1 in aerodigestive tract cancers. Clin Cancer Res 2004;10:7547–54.
48. Lu JF, Eppler SM, Wolf J, et al. Clinical pharmacokinetics of erlotinib in patients with solid tumors and exposure-safety relationship in patients with non-small cell lung cancer. Clin Pharmacol Ther 2006;80:136–45.
49. Forgacs E, Biesterveld EJ, Sekido Y, et al. Mutation analysis of the PTEN/MMAC1 gene in lung cancer. Oncogene 1998;17:1557–65.
50. Kohno T, Takahashi M, Manda R, Yokota J. Inactivation of the PTEN/MMAC1/TEP1 gene in human lung cancers. Genes Chromosomes Cancer 1998;22:152–6.